Arctic Ocean planktonic foraminifera during MIS 5: Understanding Arctic Amplification of climate change from the palaeoclimatological record

Joshua Mauss, B.S.F.S in Science, Technology, and International Affairs
Senior Honors Thesis Manuscript

Abstract

This palaeoclimatological study of the Arctic examines two sediment cores from the Arctic Ocean for planktonic foraminifera from the interglacial Marine Isotope Stage 5 (MIS 5). MIS 5 is of particular importance as it was the most recent interglacial period prior to the Holocene and provides a baseline context for understanding modern sea-ice loss and warming sea-surface temperatures. This study developed a foraminifer assemblage-based estimate of sea surface conditions by examining two Western Arctic cores, P1-93-AR-P21 (P21) from Northwind Ridge and P1-94-AR-PC9 (PC9) from Mendeleev Ridge. Twelve samples taken from each core at intervals of 5 cm correspond to MIS 5 based on preliminary age models (from 69-121 cm in P21 and 105-169 cm in PC9). Samples were washed through >63 micron sieves and the coarse fraction was split until a subset of approximately 300 foraminifers remained. Planktonic foraminifera were picked from each final subset of a sample. Six distinct morpho-species were identified, and the presence of other organisms and overall abundance of foraminifers were also noted. Four species emerged as abundant in both cores, two relatively warm water species (*Turborotalita quinqueloba* and *T. egelida*) and two cold water species that dominate today's Arctic Ocean (*Neogloboquadrina pachyderma* and *N. incompta*). *N. pachyderma* and *T. quinqueloba* were the two most prominent species during MIS 5 in both cores. *N. pachyderma* ranged from 23-75% in P21 and from 9-76% in PC9, while *T. quinqueloba* ranged from 7-65% in P21 and 16-84% in PC9. Changes in the proportional abundance of each pair of species combined were plotted against core depth to more accurately develop an age model for these cores and understand climatological trends in the Arctic Ocean during MIS 5.

Introduction

The warm climatic conditions during the last pre-Holocene interglacial period, Marine Isotope Stage 5 (MIS 5), provide an analog to present-day warming and near future projections of climate change, thus meriting further study of environmental processes during that period. MIS 5 occurred between 80,000 and 130,000 years ago as part of a cycle of cold glacials and warm interglacials during the Quaternary Period of the last 2.6 million years. MIS 5 is further subdivided into MIS 5a at the youngest end through MIS 5e at the oldest end, with MIS 5 a, c, and e representing interstadial sub-stages and b and d representing stadial substages (Pillans and Gibbard 2012). As a result, MIS 5 is very informative to present day climate as we are currently in an interglacial warm period and MIS 5 provides a recent geologic comparison where many climatic and planetary conditions are close to current conditions. Furthermore, MIS 5e specifically was about 2°C warmer than modern day, making climatic conditions during MIS 5e comparable to projections of anthropogenically forced climate change in the modern era; this similarity therefore makes MIS 5 an important time to study for both prediction of large-scale climatic trends and improving climate model (Rohling et al. 2008).

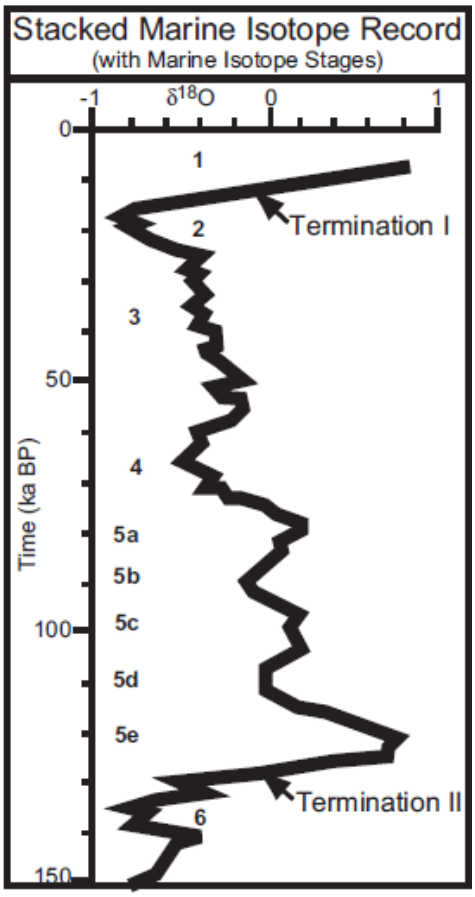

Figure 1. Temperature proxy $\delta^{18}O$ plotted from MIS 6 through present. (Reproduced from Pillans and Gibbard 2012).

Marine sediment cores have been a critical archive in paleoceanography since the mid-1900s in developing a geologic time scale to identify past climatic conditions prior to human record (Pillans and Gibbard 2012). The faunal microfossils preserved in the sedimentation record recovered by these cores reveal climatic conditions, principally sea surface temperature and salinity, through microplankton assemblage studies and proxy data recorded from the calcite shells of these species; this includes many methods, including stable oxygen isotopic composition ($\delta^{18}O$) and Mg/Ca ratios (Stuut et al. 2012).

These assemblages and proxies can be applied for a paleothermometry analysis that reconstructs sea surface temperatures (SST) and climatic conditions during past warm periods. When factoring for the sedimentation rate, planktonic foraminifera in the historical water column can reconstruct the temperature record and sea ice extent in global and regional geological studies (Farmer et al. 2011; Kinnard et al. 2011; de Vernal et al. 2013). These SST records are vital to understanding macro paleoclimatic conditions and large-scale oscillations that govern Earth's climate system (Wang et al. 2018; Lynch-Stieglitz 2017; Stranne, Jakobsson, and Björk 2014).

This study will utilize an assemblage study of planktonic (planktic) foraminifera to understand historical climatic conditions of the Arctic. Planktic foraminifers are shelled protists, typically living in the water column of marine environments, whose shell remains can be used as microfossil evidence to reconstruct past climatic conditions of the ocean they lived in through assemblage and geochemical analysis (Pados et al. 2014; O'Regan et al. 2019). The presence of other scientifically relevant fauna is noted but not the focus of this study—benthic foraminifera, ostracodes, diatoms, and radiolarians are also used in assemblage and geochemical analysis complimentary to planktonic foraminifera (Barrientos et al. 2018; Cronin et al. 2013).

Previous analysis of planktonic foraminifera assemblages in the Arctic Ocean during the Quaternary Period have revealed that *Neogloboquadrina pachyderma (s), Neogloboquadrina incompta, Turborotalita quinqueloba, Turborotalita egelida,* and *Globigerina bulloides* are geographically characteristic of the Arctic and are present in enough abundance to yield germane assemblages (Cronin et al. 2013; O'Regan et al. 2019). More specifically, the polar species *N. pachyderma* and the sub-polar species *T. quinqueloba* have been identified as significant species particularly during the last interglacial (MIS 5) in which evidence suggests that the relatively warm water species, *T. quinqueloba,* made intrusions into the Arctic Ocean (Pados and Spielhagen 2014; Pados et al. 2014).

These palaeoclimatological studies show that planktic foraminifers can be used to reconstruct sea ice patterns during warm periods including estimations of summer seasonal sea ice decline. Consequently, they provide a baseline against which we can compare to present day were sea ice is retreating in large parts of the Arctic Ocean (Kinnard et al. 2011).

Examining these palaeoceanographic conditions of the Arctic can further inform the understanding of how the Arctic interacts with the rest of Earth's climate system, especially with regards to the phenomena of Arctic Amplification (AA). During warming periods globally, high-latitude regions have been observed to exhibit accelerated changes in climate compared to the low-latitudes, which results in comparably higher temperatures in the Arctic and negative trends in sea-ice extent (Otto-Bliesner et al. 2017; Cronin et al. 2017). This phenomenon is best understood in the context of climatic feedback loops, in which the direct consequences of a climatic change either reinforce and accelerate that change (positive feedback) or counteract and reduce that change (negative feedback) (Goosse 2010). The central feedback cycle of the Arctic is the sea ice-albedo feedback, in which the climatic forcing of warming temperatures causes sea ice to melt, revealing darker water beneath and thereby reducing the overall albedo of the Arctic, thus reinforcing the original warming trend by absorbing more heat. This feedback loop is a central mechanism governing the Arctic energy budget and a factor in AA (Stranne, Jakobsson, and Björk 2014).

AA also impacts regional climates beyond the high latitudes and in turn is a factor in global climate systems. There is evidence of a correlation between reduced sea ice extent and a weakened polar vortex causing a cooling trend and severe winters in central Eurasia (Mori et al. 2019), and polar meltwater forcing is a contributor to the weakening of the Atlantic Meridional Overturning Circulation (Clark et al. 2002; Lynch-Stieglitz 2017). As current trends of sea-ice loss are unprecedented in modern times, utilizing palaeoceanographic tools can reveal

amplification behavior in previous warm periods to further our ability to understand and predict how the Arctic will behave (Kinnard et al. 2011).

Methodology

2.1 Sediment samples

Two sediment cores were selected for principal analysis over the MIS 5 region of their column: P1-93-AR-P21, cored in 1993 along the Northwind Ridge in the Arctic Ocean, and P1-94-AR-P9, cored in 1994 along the Mendeleev Ridge in the Arctic Ocean. These cores were selected for their high quality of preservation of marine fossils and record of study in other areas of the core to compare to.

One core was selected as a secondary core for reference and extra analysis if needed. This core was LOMROG12, cored in 2012 along the Lomonosov Ridge in the Arctic Ocean. Sediment from this core was washed and vialed as part of this thesis.

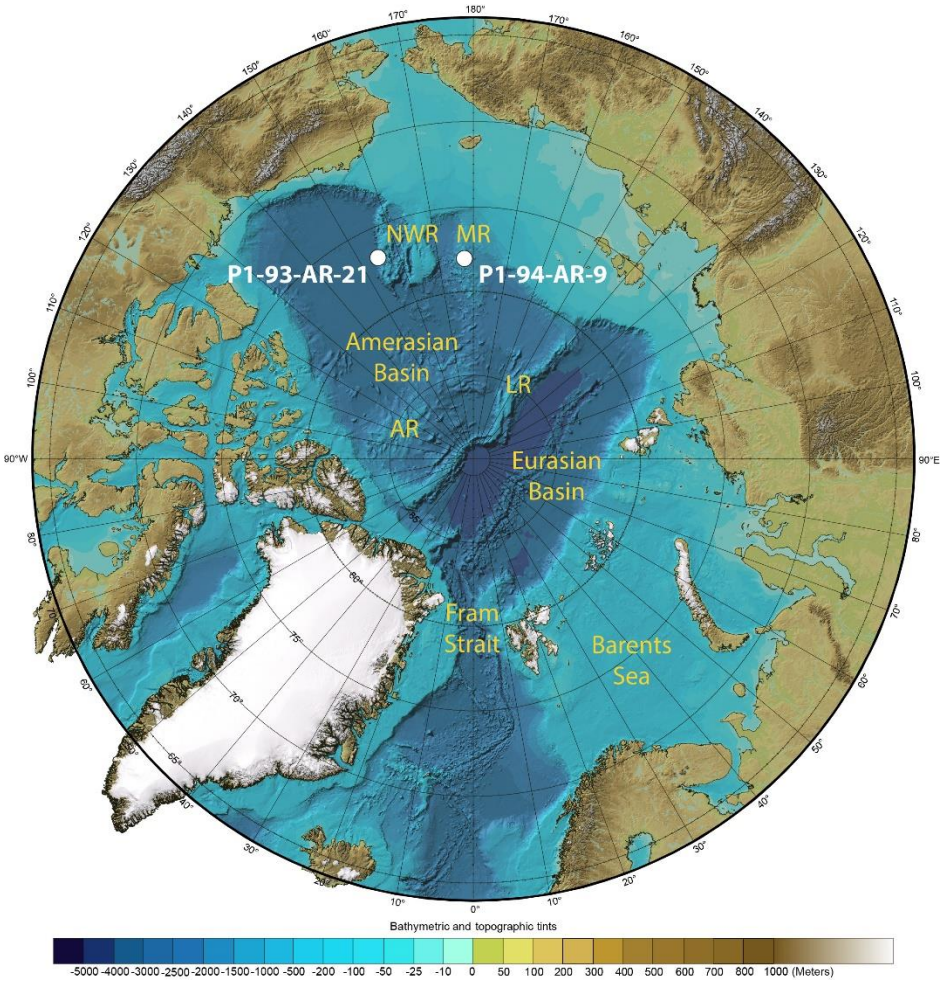

Figure 2. Bathymetric map of the Arctic Ocean with the location of marine sediment cores used in this study.

2.2 Sample preparation

The total weight of the wet sediment and its packaging were taken for each section of the sediment core before being washed. The wet sediment was then removed from the packaging, the packaging was dried and then weighed separately. A wet sediment weight was obtained for each section by subtracting the weight of the packaging from the total weight of the wet sediment and the packaging. The wet sediment was then washed in a laboratory sink through a 63μm sieve to remove extraneous very small sediments, such as clay particles, but retain the foraminifer shells. 63μm was chosen as it is the commonly accepted washing size for sediment cores at high resolution and the foraminifera found in these Arctic Ocean cores tended to be smaller and therefore required a smaller grain size sieve. The remaining wet sediment was poured through a filter paper covered funnel to remove excess water. The sediment sample was then inserted into heat resistant plastic beakers and heated in a furnace at 60°C for a minimum of 12 hours to remove any remaining moisture.

Glass vials were labeled with the section information and weighed to establish a tare weight for the dry sediment samples. The sediment samples were removed from the furnace and the sediment was swept into a vial using laboratory brushes. Any sediment that fell outside of the vial was collected by paper placed beneath and then swept into the vial. This process of catching any missing sediment was repeated at least twice for each sample. The vialed dry sediment was then weighed. The weight previously obtained was subtracted from this total weight to find the dry sediment weight.

These P21 and P9 had been previously washed following this methodology, while the LOMROG12 core was newly prepared with this methodology.

2.3 Picking planktonic foraminifera

Sediment samples were selected at an interval of five centimeters and picked for foraminifer shells under microscope (with the goal of 300 foraminifera per vial to attain a statistically representative sample). Samples clearly abundant (greater than 600) in foraminifers were divided in half using a sediment splitter. This splitting process was repeated until the sample had fewer than 600 foraminifer shells. The final subset was separated and picked for foraminifera.

The selected sample was poured over a segmented picking tray divided into a grid of five rows and nine columns for an overall number of 45 boxes. Each of the 45 boxes of the picking tray was assigned a unique random number from 1 to 45 using a random number generator. Foraminifers were picked from the tray following this random order of boxes. A laboratory slide was labeled with the section information of the sample and treated with glue to ensure foraminifers would adhere to the slide and let to dry. These slides had five rows and twelve columns for a total of 60 sample boxes. Foraminifer shells were picked from the picking tray with a wetted thin laboratory brush and placed on the slide. This process was continued until at least 300 foraminifers were selected from the picking tray.

2.4 Foraminifera identification

Foraminifera shells were identified and sorted into seven species or species groups: *Globigerinita glutinata* & *Globigerinita uvula* (combined), *G. bulloides, T. egelida, T. quinqueloba, N. pachyderma, N. incompta,* and Other. Foraminifera shells were identified from shell morphological characteristics outlined in foundational research on the taxonomy of planktonic foraminifera accompanied with scanning electron microscope (SEM) photographs. The presence and number of benthic foraminifers, ostracodes, radiolarians & diatoms (combined), and ice rafted debris (IRD) were also recorded for reference, with IRD identified simply as either present of not present. Initial results using this methodology were cross-referenced with identification results of a second researcher to confirm accuracy.

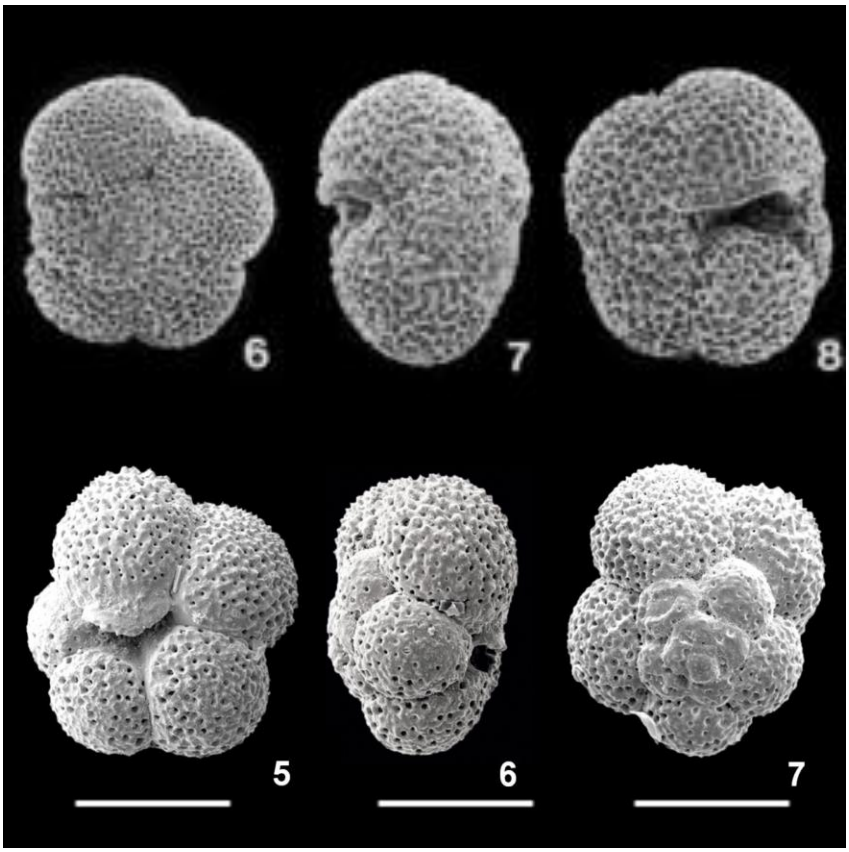

Figure 3. SEM photos of planktonic foraminifers used for identification. *N. pachyderma* (Figure 3a, top) and *T. quinqueloba* (Figure 3b, bottom) were common species.

The number of planktonic foraminifera of each species were recorded to create an assemblage for the sample. This process was repeated for each section of the sediment cores at five centimeters intervals to cover a greater length of the MIS5 region of the cores.

Results

The two piston cores (P21 and PC9) were drilled in 1993 and 1994 on the Northwind and Mendeleev Ridges (Figure 2). Consequently, these cores represent foraminifera assemblages near to the center of the Arctic Ocean off the northern coast of Alaska and north of the East Siberian Shelf respectively.(Grantz et al. 1993)

These cores were analyzed during the MIS 5 (80-130kyr) interval based on their published age models (Cronin et al. 2014; Marzen, DeNinno, and Cronin 2016). MIS 5 was characterized by

overall warm temperatures with three warm interstadial substages (5e, 5c, 5a) and two cool stadial substages (5d, 5b) as indicated by the $\delta^{18}O$ record of global foraminifers (Figure 1).

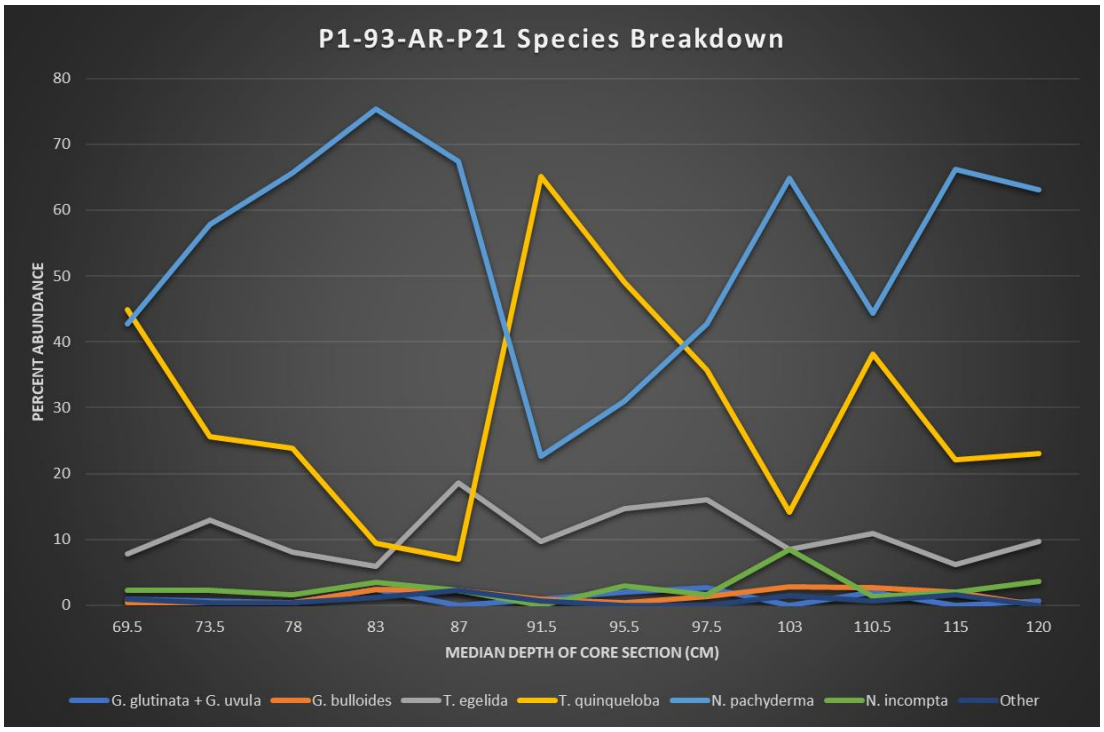

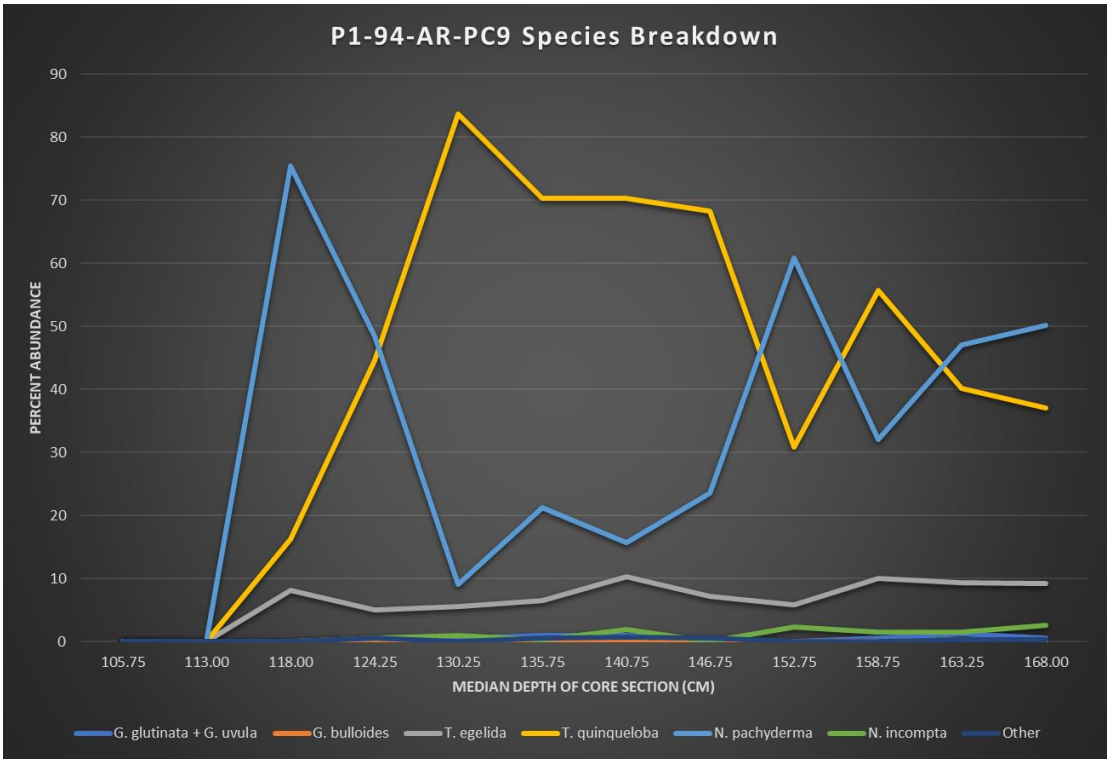

Figure 4. Percent abundance of each of six selected planktonic foraminifera species across the MIS 5 range of core P1-93-AR-P21 (Figure 4a) and core P1-94-AR-PC9 (Figure 4b).

Assemblages of planktonic foraminifera were taken at intervals of five centimeters over the sections of each core that were deposited during MIS 5 according to the age model of the core. Throughout both cores the two most common species were *N. pachyderma* and *T. quinqueloba*, with the next most common species being *T. egelida* and *N. incompta* in that order. Thus, the characteristic species of this region during MIS 5 appear to be *N. pachyderma* and *T. quinqueloba*.

During the MIS 5 interval in both cores, *N. pachyderma* was the most abundant species during MIS 5d and 5b, *T. quinqueloba* the most abundant species in MIS 5c and these two species were similar in their abundances and the two were the most abundant amongst any other species. In MIS 5a this phenomenon of comparative abundance of *N. pachyderma* and *T. quinqueloba* was repeated in core P21, but the MIS 5a section of core PC9 was barren of all planktonic foraminifera.

No other species was either in high abundance displayed a distinct pattern throughout the course of MIS 5. *T. egelida*, the overall third most abundant species displayed higher variability in core P21 than PC9, but not in a way that suggested a meaningful pattern. *N. incompta*, the fourth most abundant species displayed little variability in either core with the exception of a brief spike during MIS 5d which is unlikely to be significant due to the relatively low abundance of this species to compare thorough the rest of this section of the two cores.

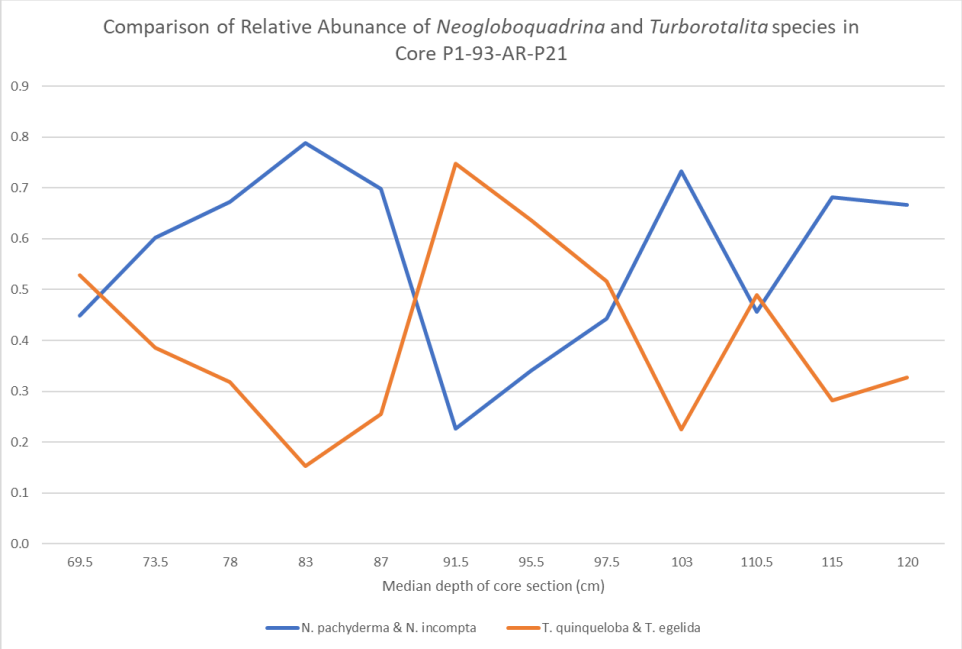

Figure 5. Comparison of the relative abundances of species of the colder water *Neogloboquadrina* genus and the warmer water *Turborotalita* genus. Core P1-93-AR-P21 (Figure 5a) and core P1-94-AR-PC9 (Figure 5b).

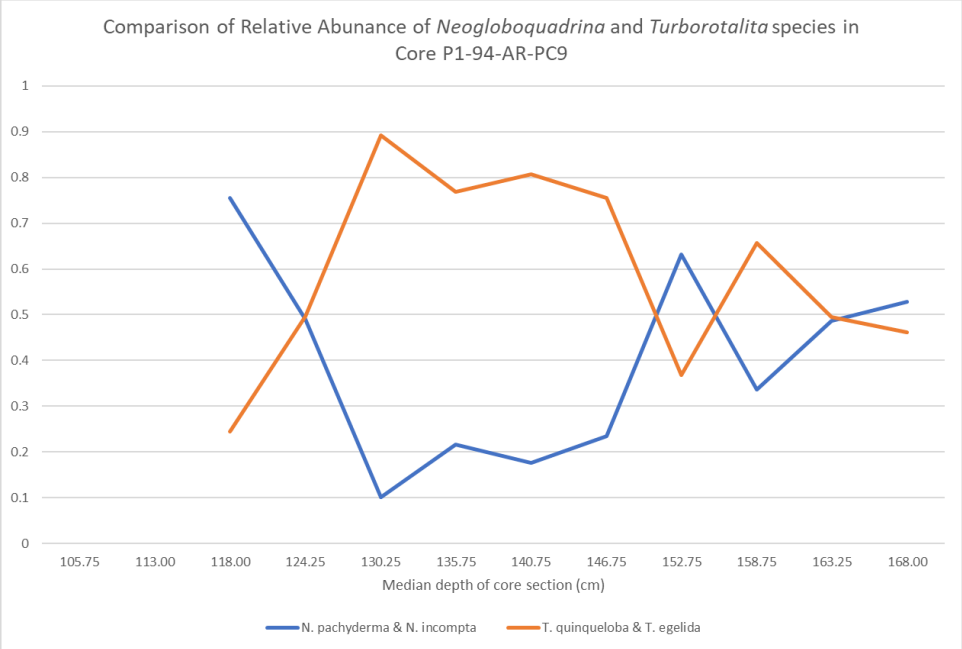

The patterns of *N. pachyderma* and *T. quinqueloba* are the most notable on a species level, and further information can also be seen by breaking down the data by the two most abundant genera—the genus *Neogloboquadrina* which typically more is adapted to colder waters and the *Turborotalita* genus which is typically more adapted to warmer waters. When doing this for both cores we see a distinct increase in the relative proportion of species of the *Turborotalita* genus at depths of the core associated with MIS 5e, 5c (both cores), and 5a (only P21), while seeing decreases in these same species during sections associated with MIS 5d and 5b (both cores). The reverse of this pattern is evident among species of the genus *Neogloboquadrina*, which saw decreases in relative proportions during MIS 5e, 5c (both cores), and 5a (only P21), while seeing increases in relative proportions during MIS 5d and 5b (both cores).

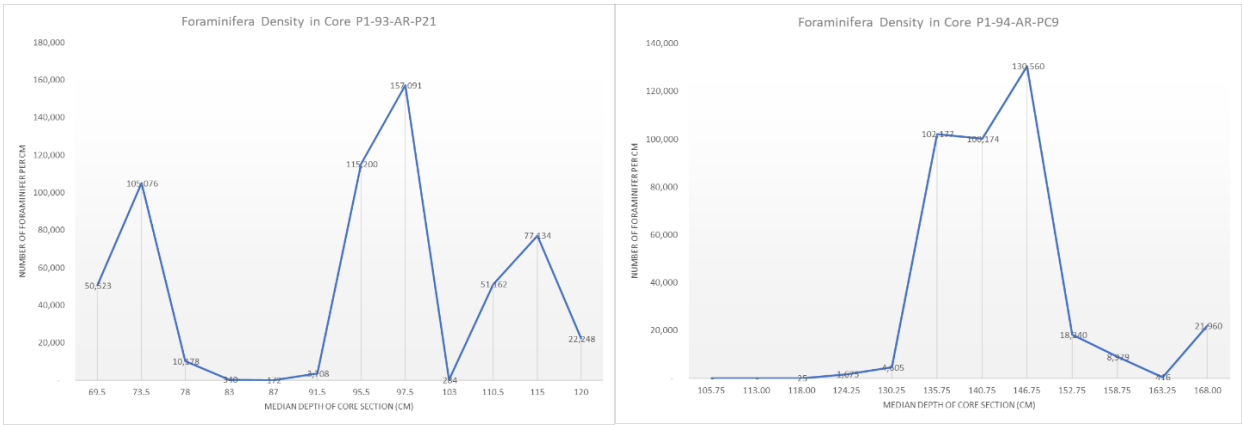

Figure 6. Overall density of planktonic foraminifera species in sections of both cores. Core P1-93-AR-P21 (Figure 6a) and core P1-94-AR-PC9 (Figure 6b).

Examining the overall abundance of planktonic foraminifera through the MIS 5 section of each core, the highest peak occurred in core P21 at ~108.5kya with an estimated number of planktic foraminifera per centimeter of the core at this section around 157,000. Core PC9 similarly saw its peak around ~111.8kya with an estimated 131,000 planktic foraminifera per centimeter of the core at that section. Both of these times are approximately consistent with the start of the MIS 5c substage.

At a further level of analysis, we find a divergence in estimated total planktic foraminifer abundance between the two cores. Core P21 reinforces the earlier patterns found in the assemblages of three significant increases in foraminifera abundances during the warm substages of 5e, 5c, and 5a, with 5c again being the section of largest increase in abundance. Meanwhile, core PC9 displays only a single notable increase in planktic foraminifera abundance during the MIS 5c portion of the core, while being barren during the MIS 5a portion and only having a very slight increase in the presence of foraminifera during MIS 5e.

Discussion

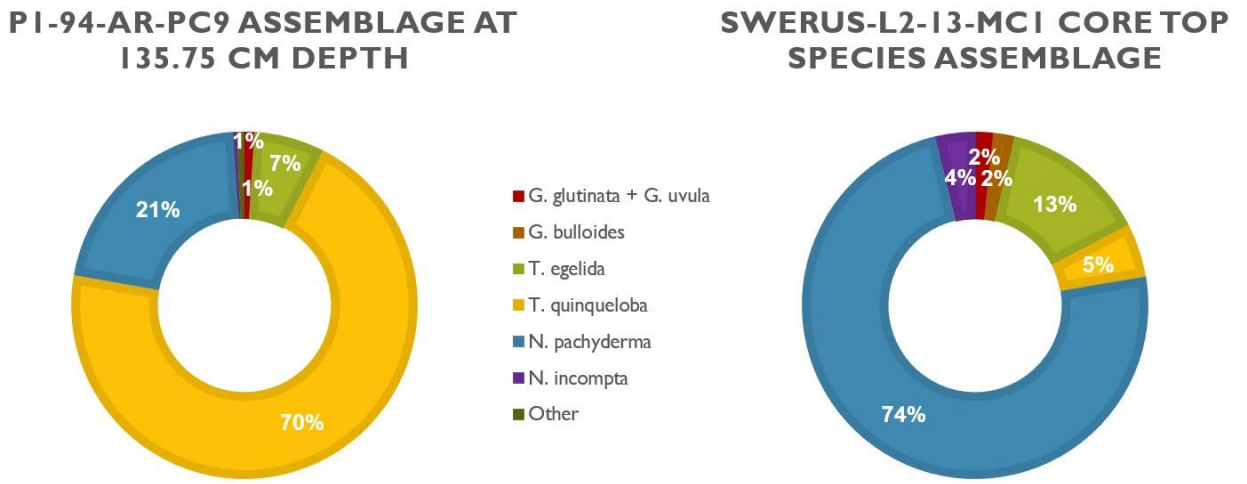

Figure 7. Comparison of planktic foraminifera species assemblages between the MIS 5 section of core P1-94-AR-PC9 from 135-136.5 cm (Figure 7a) and the SWERUS-L2-13-MC1 modern core top (Figure 7b).

Modern arctic planktic foraminifera assemblages are regularly dominated by the presence of *N. pachyderma*. This species routinely accounts for the majority of planktonic foraminifera at many locations in the Arctic Ocean, which is reflected in reference core top data. *T. egelida* is frequently the next most abundant species in modern assemblages and is a common indicator of warmer sea surface temperatures. However, the assemblages analyzed from these cores indicate that not only was *T. quinqueloba* routinely the second most abundant species when *N. pachyderma* was most abundant, but there were many occurrences in the sedimentary record where *T. quinqueloba* was the most abundant species in the assemblage by far. The comparatively high abundance of *T. quinqueloba* throughout the MIS 5 interval of these cores, especially in comparison to other intervals, suggest that *T. quinqueloba* is a characteristic species of MIS 5 in the Arctic. This has added relevance as this species appears to respond heavily to presumed changes in SST during the MIS 5 period.

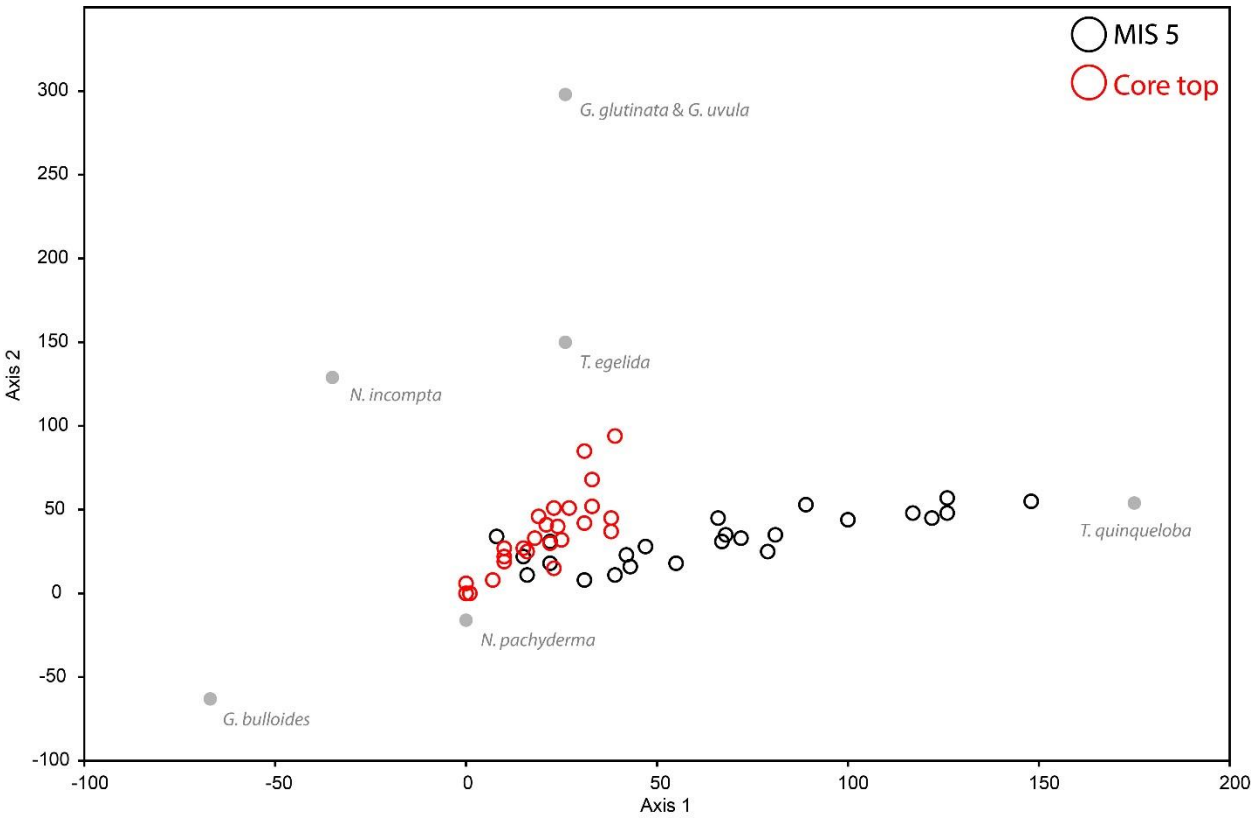

Figure 8. Plot of detrended correspondence analysis (DCA) between modern core top assemblages (MIS 1) and the assemblages from cores P1-93-AR-P21 and P1-94-AR-PC9 over the MIS 5 interval.

The twenty-four assemblages from MIS 5 were compared with twenty-six assemblages from core tops taken from Arctic Ocean sediment cores. A detrended correspondence analysis (DCA) was taken between the two groups, analyzing them along the axes of the same six species of planktonic foraminifera. Two separate trends emerged between the MIS 5 and MIS 1 assemblages. Assemblages from MIS 5, as previously discussed, trended principally between (*N. pachyderma* and *T. quinqueloba* while core top assemblages trended principally between *N. pachyderma* and *T. egelida*. Reinforcing these different trends is the evidence that there is almost no overlap between these two clusters aside from a small number of MIS 5 assemblages one the edge of the MIS 5 cluster that overlap into the cluster of modern assemblages.

The lack of overlap between these two clusters indicates that significant sea surface temperature estimates cannot be derived from these planktonic foraminifera assemblages alone. The likely reason for this significant divergence in assemblages is the warmer temperatures of the Last Interglacial likely prompted a reduced sea ice extent in the Arctic that was more favorable to warmer water foraminifera species to the extent of making the two assemblages incomparable. This extreme divergence between modern assemblages and assemblages from peak warm periods of MIS 5 likely indicate ice-free conditions that allowed warm water foraminifers, particularly *T. quinqueloba*, to thrive.

Additionally, these MIS 5 intervals indicate a greater proportion of warm water foraminifers in a region of the Arctic generally characterized by comparatively less abundance of warm water

foraminifers in modern assemblages. This could be indicative of an overall significantly warmer Arctic during MIS 5, a different regional pattern of Arctic Amplification than present patterns, or both. Combined with the sharp differences in assemblages between peaks of warm foraminifer species abundance, the data provides evidence that AA trends are more likely to be nonlinear with respect to general climatic forcing approximated by global mean temperature.

These results also suggest that the current age models of P1-93-AR-P21 and P1-94-AR-PC9 ought to be reevaluated. The primary factor in this conclusion is the apparent greater abundance of warm water foraminifers over the MIS 5c interval of both cores according to current age models compared to the abundances of these species over the significantly warmer MIS 5e interval in the same cores. Further, the low abundance of foraminifers over the MIS 5a interval in core P1-94-AR-PC9 may be related to uncertainty in the age model.

Conclusion

Planktonic foraminifera assemblages from the P1-93-AR-P21 and P1-94-AR-PC9 Arctic Ocean sediment cores suggest that *T. quinqueloba* may be useful as a characteristic species for warm climatological conditions during the Last Interglacial. This species preference for warm water conditions additionally suggests that the age models of these two cores should be revised to more accurately place the timing of MIS 5 substage peaks in the sedimentary record.

These high abundance of warm water species at peaks during MIS 5 suggests that climatological conditions in the Arctic were considerably warmer than present day, supporting higher sea surface temperatures and reduced sea ice extent. Compounded with sharp shifts in species abundance between peaks, this evidence supports a nonlinear view of Arctic Amplification. This evidence would suggest Arctic would warm at a more rapid rate than global climatological forcing. However, it remains ambiguous as to whether exponential warming in the Arctic during MIS 5 is measurably distinct from exponential warming trends globally during the same time.

Should the precedent established during MIS 5 by these cores be applied to modern climatic trends in the Arctic, exponential trends in reduction of sea ice extent and increases in sea surface temperatures can be expected to continue. Consistent with estimations that the warmest portions of MIS 5 were 2°C warmer than pre-industrial conditions, should similar global conditions of 2°C warming occur this evidence suggest seasonally ice-free conditions in the Arctic are possible as consistent with assemblages of ~80% warm water foraminifer species such as *T. quinqueloba.*

Acknowledgements
Research was made possible by support from the USGS Florence Bascom Geoscience Center and the Georgetown University STIA Department. Foremost thanks to Dr. Thomas Cronin, Laura Gemery, and Alexa Regnier for their support of this research. Additional thanks to Dr. Emily Mendenhall, Dr. Marci Robinson, Dr. Jessica Rodysill, Anna Ruefer, and members of the Florence Bascom Geoscience Center team.

References

Barrientos, Natalia, Caroline H. Lear, Martin Jakobsson, Christian Stranne, Matt O'Regan, Thomas M. Cronin, Alexandr Y. Gukov, and Helen K. Coxall. 2018. "Arctic Ocean Benthic Foraminifera Mg/Ca Ratios and Global Mg/Ca-Temperature Calibrations: New Constraints at Low Temperatures." *Geochimica et Cosmochimica Acta* 236 (September): 240–59. https://doi.org/10.1016/j.gca.2018.02.036.

Cimoli, Emiliano, Klaus M Meiners, Lars Chresten Lund-Hansen, and Vanessa Lucieer. 2017. "Spatial Variability in Sea-Ice Algal Biomass: An under-Ice Remote Sensing Perspective" 28 (4): 29.

Clark, Peter U., Nicklas G. Pisias, Thomas F. Stocker, and Andrew J. Weaver. 2002. "The Role of the Thermohaline Circulation in Abrupt Climate Change." *Nature* 415 (6874): 863–69. https://doi.org/10.1038/415863a.

Cronin, T. M., G. S. Dwyer, E. K. Caverly, J. Farmer, L. H. DeNinno, J. Rodriguez-Lazaro, and L. Gemery. 2017. "Enhanced Arctic Amplification Began at the Mid-Brunhes Event ~400,000 Years Ago." *Scientific Reports* 7 (1): 14475. https://doi.org/10.1038/s41598-017-13821-2.

Cronin, T.M., L.H. DeNinno, L. Polyak, E.K. Caverly, R.Z. Poore, A. Brenner, J. Rodriguez-Lazaro, and R.E. Marzen. 2014. "Quaternary Ostracode and Foraminiferal Biostratigraphy and Paleoceanography in the Western Arctic Ocean." *Marine Micropaleontology* 111 (September): 118–33. https://doi.org/10.1016/j.marmicro.2014.05.001.

Cronin, T.M., L. Polyak, D. Reed, E.S. Kandiano, R.E. Marzen, and E.A. Council. 2013. "A 600-Ka Arctic Sea-Ice Record from Mendeleev Ridge Based on Ostracodes." *Quaternary Science Reviews* 79 (November): 157–67. https://doi.org/10.1016/j.quascirev.2012.12.010.

Farmer, Jesse R., Thomas M. Cronin, Anne de Vernal, Gary S. Dwyer, Lloyd D. Keigwin, and Robert C. Thunell. 2011. "Western Arctic Ocean Temperature Variability during the Last 8000 Years: ARCTIC OCEAN TEMPERATURE VARIABILITY." *Geophysical Research Letters* 38 (24): n/a-n/a. https://doi.org/10.1029/2011GL049714.

Gasson, Edward G. W., Robert M. DeConto, David Pollard, and Chris D. Clark. 2018. "Numerical Simulations of a Kilometre-Thick Arctic Ice Shelf Consistent with Ice Grounding Observations." *Nature Communications* 9 (1): 1510. https://doi.org/10.1038/s41467-018-03707-w.

Goosse, H. 2005. "Modelling the Climate of the Last Millennium: What Causes the Differences between Simulations?" *Geophysical Research Letters* 32 (6): L06710. https://doi.org/10.1029/2005GL022368.

Goosse, H., O. Arzel, C. M. Bitz, A. de Montety, and M. Vancoppenolle. 2009. "Increased Variability of the Arctic Summer Ice Extent in a Warmer Climate." *Geophysical Research Letters* 36 (23): L23702. https://doi.org/10.1029/2009GL040546.

Goosse, H, O Arzel, J Luterbacher, M E Mann, H Renssen, N Riedwyl, A Timmermann, E Xoplaki, and H Wanner. 2006. "The Origin of the European 'Medieval Warm Period.'" *Clim. Past*, 15.

Goosse, Hugues. 2010. “Degrees of Climate Feedback.” *Nature* 463 (7280): 438–39. https://doi.org/10.1038/463438a.

Goosse, Hugues, and Hans Renssen. 2005. “A Simulated Reduction in Antarctic Sea-Ice Area since 1750: Implications of the Long Memory of the Ocean.” *International Journal of Climatology* 25 (5): 569–79. https://doi.org/10.1002/joc.1139.

Grantz, Arthur, P. E. Hart, R. L. Phillips, Michael McCormick, R. G. Perkin, Ruth Jackson, Alan Gagmon, Shusun Li, Carl Byers, and Schwartz. 1993. “Cruise Report and Preliminary Results U.S. Geological Survey Cruise P1-93 ARNorthwind Ridge and Canada Basin, Arctic OceanAboard USCGC POLAR STARAugust 16 - September 15, 1993.” Open-File Report. Open-File Report.

Helmens, Karin F. 2014. “The Last Interglacial–Glacial Cycle (MIS 5–2) Re-Examined Based on Long Proxy Records from Central and Northern Europe.” *Quaternary Science Reviews* 86 (February): 115–43. https://doi.org/10.1016/j.quascirev.2013.12.012.

IPCC. 2013. “IPCC Summary for Policymakers 2013.”

Kinnard, Christophe, Christian M. Zdanowicz, David A. Fisher, Elisabeth Isaksson, Anne de Vernal, and Lonnie G. Thompson. 2011. “Reconstructed Changes in Arctic Sea Ice over the Past 1,450 Years.” *Nature* 479 (7374): 509–12. https://doi.org/10.1038/nature10581.

Lynch-Stieglitz, Jean. 2017. “The Atlantic Meridional Overturning Circulation and Abrupt Climate Change.” *Annual Review of Marine Science* 9 (1): 83–104. https://doi.org/10.1146/annurev-marine-010816-060415.

Marzen, Rachel E., Lauren H. DeNinno, and Thomas M. Cronin. 2016. “Calcareous Microfossil-Based Orbital Cyclostratigraphy in the Arctic Ocean.” *Quaternary Science Reviews* 149 (October): 109–21. https://doi.org/10.1016/j.quascirev.2016.07.004.

Mori, Masato, Yu Kosaka, Masahiro Watanabe, Hisashi Nakamura, and Masahide Kimoto. 2019. “A Reconciled Estimate of the Influence of Arctic Sea-Ice Loss on Recent Eurasian Cooling.” *Nature Climate Change* 9 (2): 123–29. https://doi.org/10.1038/s41558-018-0379-3.

Nash, David J., and Sarah E. Metcalfe. 2012. “Past Environmental Changes, Future Environmental Challenges.” In *Quaternary Environmental Change in the Tropics*, edited by Sarah E. Metcalfe and David J. Nash, 392–411. Chichester, UK: John Wiley & Sons, Ltd. https://doi.org/10.1002/9781118336311.ch11.

O’Regan, Matt, Helen K. Coxall, Thomas M. Cronin, Richard Gyllencreutz, Martin Jakobsson, Stefanie Kaboth, Ludvig Löwemark, Steffen Wiers, and Gabriel West. 2019. “Stratigraphic Occurrences of Sub-Polar Planktic Foraminifera in Pleistocene Sediments on the Lomonosov Ridge, Arctic Ocean.” *Frontiers in Earth Science* 7 (April): 71. https://doi.org/10.3389/feart.2019.00071.

Otto-Bliesner, Bette L., Pascale Braconnot, Sandy P. Harrison, Daniel J. Lunt, Ayako Abe-Ouchi, Samuel Albani, Patrick J. Bartlein, et al. 2017. “The PMIP4 Contribution to CMIP6 – Part 2:

Two Interglacials, Scientific Objective and Experimental Design for Holocene and Last Interglacial Simulations." *Geoscientific Model Development* 10 (11): 3979–4003. https://doi.org/10.5194/gmd-10-3979-2017.

Pados, T., R. F. Spielhagen, D. Bauch, H. Meyer, and M. Segl. 2014. "Oxygen and Carbon Isotope Composition of Modern Planktic Foraminifera and Near-Surface Waters in the Fram Strait (Arctic Ocean) – a Case-Study." *Biogeosciences Discussions* 11 (6): 8635–72. https://doi.org/10.5194/bgd-11-8635-2014.

Pados, Theodora, and Robert F. Spielhagen. 2014. "Species Distribution and Depth Habitat of Recent Planktic Foraminifera in Fram Strait, Arctic Ocean." *Polar Research* 33 (1): 22483. https://doi.org/10.3402/polar.v33.22483.

Pillans, B., and P. Gibbard. 2012. "The Quaternary Period." In *The Geologic Time Scale*, 979–1010. Elsevier. https://doi.org/10.1016/B978-0-444-59425-9.00030-5.

Rohling, E. J., G. L. Foster, K. M. Grant, G. Marino, A. P. Roberts, M. E. Tamisiea, and F. Williams. 2014. "Sea-Level and Deep-Sea-Temperature Variability over the Past 5.3 Million Years." *Nature* 508 (7497): 477–82. https://doi.org/10.1038/nature13230.

Rohling, E. J., K. Grant, Ch. Hemleben, M. Siddall, B. A. A. Hoogakker, M. Bolshaw, and M. Kucera. 2008. "High Rates of Sea-Level Rise during the Last Interglacial Period." *Nature Geoscience* 1 (1): 38–42. https://doi.org/10.1038/ngeo.2007.28.

Routson, Cody C., Nicholas P. McKay, Darrell S. Kaufman, Michael P. Erb, Hugues Goosse, Bryan N. Shuman, Jessica R. Rodysill, and Toby Ault. 2019. "Mid-Latitude Net Precipitation Decreased with Arctic Warming during the Holocene." *Nature* 568 (7750): 83–87. https://doi.org/10.1038/s41586-019-1060-3.

Seidenkrantz, Marit-Solveig, Anne de Vernal, and Hugues Goosse. n.d. "Northern Hemisphere Sea-Ice Cover during the Holocene – Proxy Data Reconstruction and Modelling," 1.

Stranne, Christian, Martin Jakobsson, and Göran Björk. 2014. "Arctic Ocean Perennial Sea Ice Breakdown during the Early Holocene Insolation Maximum." *Quaternary Science Reviews* 92 (May): 123–32. https://doi.org/10.1016/j.quascirev.2013.10.022.

Stuut, Jan-Berend W, Matthias Prange, Ute Merkel, and Silke Steph. 2012. "3.1 Tropical Oceans in the Global Climate System." In *Quaternary Environmental Change in the Tropics*, 45. Chichester, UK: John Wiley & Sons, Ltd.

Telesiński, Maciej M., Henning A. Bauch, and Robert F. Spielhagen. 2018. "Causes and Consequences of Arctic Freshwater Routing into the Nordic Seas during Late Marine Isotope Stage 5: ARCTIC FRESHWATER ROUTING INTO THE NORDIC SEAS DURING LATE MIS 5." *Journal of Quaternary Science* 33 (7): 794–803. https://doi.org/10.1002/jqs.3060.

Vernal, Anne de, Rainer Gersonde, Hugues Goosse, Marit-Solveig Seidenkrantz, and Eric W. Wolff. 2013. "Sea Ice in the Paleoclimate System: The Challenge of Reconstructing Sea Ice from

Proxies – an Introduction." *Quaternary Science Reviews* 79 (November): 1–8. https://doi.org/10.1016/j.quascirev.2013.08.009.

Wang, Rujian, Leonid Polyak, Wenshen Xiao, Li Wu, Taoliang Zhang, Yechen Sun, and Xiaomei Xu. 2018. "Late-Middle Quaternary Lithostratigraphy and Sedimentation Patterns on the Alpha Ridge, Central Arctic Ocean: Implications for Arctic Climate Variability on Orbital Time Scales." *Quaternary Science Reviews* 181 (February): 93–108. https://doi.org/10.1016/j.quascirev.2017.12.006.

Appendix

Table 1. Data table for foraminifera assemblages collected from core P1-93-AR-P21.

P1-93-AR-P21 1470 m	Upper Depth	Lower Depth	Median Depth (cm)	Age (kya)	Num. Splits	Max Box	Comments	G. glutinata + G. uvula	G. bulloides	T. egelida	T. quinqueloba	N. pachyderma	N. incompta	Other	Total	Benthics	Ostracodes	Radiolarians & Diatoms	IRD	Source
P1-93-AR-P21	**69**	**70**	**69.5**	83.2	**7**	**35**	total 304, roughly even pachys and quinqeloba, perhaps sli	3	1	24	138	131	7	3	**307**					**LD Menlo**
P1-93-AR-P21	**73**	**74**	**73.5**	86.8	**8**	**33**	ninth pick, large benthics	2	1	39	77	174	7	1	**301**	8	0	0	Y	**LD Menlo**
P1-93-AR-P21	**77**	**79**	**78**	90.9	**6**	**44**	sixth pick, very bad preservation	1	1	25	74	204	5	1	**311**	1	0	0	Y	**TC Menlo**
P1-93-AR-P21	**82**	**84**	**83**	95.4	**3**	**45**	tenth pick, few forams	2	2	5	8	64	3	1	**85**	0	0	0	Y	**TC Menlo**
P1-93-AR-P21	**86**	**88**	**87**	99.0	**3**	**45**	seventh pick, bad preservation, very few forams	0	1	8	3	29	1	1	**43**	0	0	0	Y	**TC Menlo**
P1-93-AR-P21	**91**	**92**	**91.5**	103.1	**3**	**30**	fourth pick, separated pachys from quin and egelida	3	3	30	201	70	0	2	**309**	0	0	0	Y	**LD Menlo**
P1-93-AR-P21	**95**	**96**	**95.5**	106.7	**7**	**15**	Second pick for Mauss	6	1	44	147	93	9	0	**300**	5	0	0	Y	**LD Menlo**
P1-93-AR-P21	**97**	**98**	**97.5**	108.5	**7**	**11**	First pick for Mauss, slide dropped at end	8	4	48	107	128	5	0	**300**	8	0	0	Y	**LD Menlo**
P1-93-AR-P21	**102**	**104**	**103**	113.5	**3**	**45**	eighth pick, poor preservation, very few forams	0	2	6	10	46	6	1	**71**	1	0	0	Y	**TC Menlo**
P1-93-AR-P21	**110**	**111**	**110.5**	120.3	**6**	**17**	Third pick, slide sorted by species	6	8	33	115	134	4	2	**302**	22	0	0	Y	**LD Menlo**
P1-93-AR-P21	**114**	**116**	**115**	124.4	**8**	**23**	firfth pick, sorted by species, 15 per box	0	6	19	68	204	6	5	**308**	8	0	0	Y	**TC Menlo**
P1-93-AR-P21	**119**	**121**	**120**	128.9	**7**	**40**	expanding the selection region	2	0	30	71	195	11	0	**309**	1	0	0	Y	**WHOI/Poore**

Table 2. Data table for foraminifera assemblages collected from core P1-94-AR-P9.

P1-94-AR-PC9 1399 m	Upper Depth	Lower Depth	Median Depth (cm)	Age (kya)	Num. Splits	Max Box	Comments	G. glutinata + G. uvula	G. bulloides	T. egelida	T. quinqueloba	N. pachyderma	N. incompta	Other	Total	Bethics	Ostracodes	Radiolarians & Diatoms	IRD	Source
P1-94-AR-PC9	**105.0**	**106.5**	**105.75**	81.7	0	0	BARREN	0	0	0	0	0	0	0	**0**	0	0	0	N	**Menlo**
P1-94-AR-PC9	**112.0**	**114.0**	**113.00**	87.0	0	0	BARREN	0	0	0	0	0	0	0	**0**	0	0	0	N	**Poore**
P1-94-AR-PC9	**117.0**	**119.0**	**118.00**	90.7	0	45	7th pick, very few forams, orange grains?	0	0	4	8	37	0	0	**49**	0	0	0	N	**Menlo**
P1-94-AR-PC9	**123.5**	**125.0**	**124.25**	95.3	3	45	6th pick, picked to edges of tray	1	1	16	140	152	2	2	**314**	8	0	0	Y	**Menlo**
P1-94-AR-PC9	**129.5**	**131.0**	**130.25**	99.7	3	16	5th pick, unexpectedly large number of forams	2	0	17	257	28	3	0	**307**	3	0	1	Y	**Menlo**
P1-94-AR-PC9	**135.0**	**136.5**	**135.75**	103.7	8	23	combined from three size ranges from WHOI, abundant forams	3	0	20	215	65	1	2	**306**	8	0	0	Y	**Poore**
P1-94-AR-PC9	**140.0**	**141.5**	**140.75**	107.4	8	23	first pick of this core, abundant forams	3	0	31	211	47	6	2	**300**	6	0	0	Y	**Menlo**
P1-94-AR-PC9	**146.0**	**147.5**	**146.75**	111.8	9	36	2nd, abundant	1	0	22	209	72	0	2	**306**	11	0	0	Y	**Menlo**
P1-94-AR-PC9	**152.0**	**153.5**	**152.75**	116.2	6	32	3rd, semi-abundant	0	0	18	94	185	7	0	**304**	9	0	0	Y	**Menlo**
P1-94-AR-PC9	**158.0**	**159.5**	**158.75**	120.6	4	17	8th, abundant forams	2	0	32	177	102	5	0	**318**	4	0	0	Y	**Poore/WHOI**
P1-94-AR-PC9	**162.5**	**164.0**	**163.25**	123.9	0	23	9th, small amount of sediment	4	1	30	128	150	5	1	**319**	5	0	0	Y	**Poore**
P1-94-AR-PC9	**167.0**	**169.0**	**168.00**	127.4	7	40	very abundant forams	2	0	28	113	153	8	1	**305**					**Menlo**